Synthesis, characterization and dye removal ability of high capacity polymeric adsorbent: Polyaminoimide homopolymer

Niyaz Mohammad Mahmoodi [a,*], Farhood Najafi [b], Shooka Khorramfar [a,c], Farrokhlegha Amini [a], Mokhtar Arami [c]

[a] Department of Environmental Research, Institute for Color Science and Technology, Tehran, Iran
[b] Department of Resin and Additives, Institute for Color Science and Technology, Tehran, Iran
[c] Textile Engineering Department, Amirkabir University of Technology, Tehran, Iran

ABSTRACT

In this paper, polyaminoimide homopolymer (PAIHP) was synthesized and its dye removal ability was investigated. Physical characteristics of PAIHP were studied using Fourier transform infrared (FTIR) and scanning electron microscopy (SEM). Direct Red 31 (DR31), Direct Red 23 (DR23), Direct Black 22 (DB22) and Acid Blue 25 (AB25) were used as model compounds. The kinetic and isotherm of dye adsorption were studied. The effect of operational parameter such as adsorbent dosage, pH and salt on dye removal was evaluated. Adsorption kinetic of dyes followed pseudo-second order kinetics. The maximum dye adsorption capacity (Q_0) of PAIHP was 6667 mg/g, 5555 mg/g, 9090 mg/g and 5882 mg/g for DR31, DR23, DB22 and AB25, respectively. It was found that adsorption of DR31, DR23, DB22 and AB25 onto PAIHP followed with Langmuir isotherm. Dye desorption tests (adsorbent regeneration) showed that the maximum dye release of 90% for DR31, 86% for DR23, 87% for DB22 and 90% for AB25 were achieved in aqueous solution at pH 12. The results showed that the PAIHP as a polymeric adsorbent with high dye adsorption capacity might be a suitable alternative to remove dyes from colored wastewater.

© 2011 Elsevier B.V. All rights reserved.

1. Introduction

The presence of organic dyes in natural waterways is aesthetically undesirable and causes annoyance to the organisms because it reduces the sunlight penetration and depletes the dissolved oxygen. Some dyes have potential to release the toxic, mutagenic and carcinogenic materials. Dyes, especially soluble dyes can escape from conventional wastewater treatment because they are generally designed to withstand physico-chemical and biological degradation. Industries related with dyeing such as textile consume in their processes large amounts of water. The more stringent laws adapted to wastewater discharges motivated industries to treat their wastewater using effective method [1–5].

Adsorption is the effective and simple method to remove pollutants from wastewater. Several materials such as agricultural wastes, natural compounds, activated carbon, etc. were used as adsorbents [6–14]. They tend to remove pollutants indiscriminately, making it difficult to selectively recover certain pollutants

for reuse. The low-cost adsorbents are produced on the basis of low-cost materials or even from waste and seem economically attractive for practical application. However, further improvement of their adsorption capacities, mechanical strength, and other properties need for wide application [14].

Polymeric adsorbents have been emerging as potential alternative to traditional adsorbents in terms of their vast surface area, perfect mechanical rigidity, adjustable surface chemistry and pore size distribution, and feasible regeneration under mild conditions [14]. Generally, polymeric adsorbents can effectively remove different organic and inorganic pollutants. To improve adsorption capacity of a polymeric adsorbent toward pollutants such as organics and heavy metal ions, surface modification or functionalization has proved to be an effective method because of the specific interaction of functional groups bound to the polymeric matrixes with the target pollutants [14–16]. Several polymeric adsorbents have been proposed and studied for their ability to remove dyes [17–20] (Table 1).

A literature review showed that polyaminoimide homopolymer (PAIHP) was not used to remove dyes. In this paper, PAIHP was synthesized and characterized and its dye adsorption ability was studied. Direct Red 31 (DR31), Direct Red 23 (DR23), Direct Black 22 (DB22) and Acid Blue 25 (AB25) were used as model compounds

Table 1
Adsorption capacities of polymeric adsorbents to remove dyes.

Polymeric adsorbent	Adsorbate	Q_0 (mg/g)	Ref.
Poly(glycidylmethacrylate) grafted on a cross-linked acrylate based resin	Crystal violet	77	[17]
	Basic fuchsine	127	[17]
ZCH-101	Methylene blue	21	[18]
	Reactive orange X-GN	233	[18]
Functionalized resin	Reactive brilliant blue KN-R	28	[19]
Amberlite XAD-4	Malachite Green	899	[20]
	Methyl Green	1117	
Amberlite XAD-2	Malachite Green	884	
	Methyl Green	1122	
PAIHP	Direct Red 31	6667	Present study
	Direct Red 23	5555	
	Direct Black 22	9090	
	Acid Blue 25	5882	

in this work. Physical characteristics of PAIH were investigated. The isotherm and kinetic of dye adsorption was studied in details. The effect of operational parameter such as adsorbent dosage, pH and salt on dye removal was evaluated. In addition, dye desorption tests were done to study the adsorbent regeneration.

2. Materials and methods

2.1. Materials

Direct Red 31 (DR31), Direct Red 23 (DR23), Direct Black 22 (DB22) and Acid Blue 25 (AB25) were obtained from Ciba and used without further purification. The chemical structure of dyes was shown in Fig. 1. All other chemicals were of analytical grade and obtained from Merck.

2.2. Synthesis of PAIHP

Polyaminoimide homopolymer was synthesized in our laboratory (Fig. 2). Polyaminoimide was synthesized by addition of maleic anhydride (9.8 g, 0.1 mol) slowly to solution of ethylene diamine (9 g, 0.15 mol) in distilled water (20 mL). Then, solution was heated to 120 °C for 1 h, until water (20 mL) was removed and ethylene diamine connects to maleic anhydride by opening of anhydride ring. The next step, unsaturated monomer of aminoimide was prepared by heating to 140 °C for 2 h. The final step, unsaturated monomer aminoimide was homopolymerized in the presence of ammonium persulfate (0.1% (w) monomer, 0.014 g) as catalyst in 30 mL distilled water in 85 °C for 2 h. Polyaminoimide was purified by sedimentation in diethyl ether, and then powder was filtered and dried in 40 °C for 2 h in vacuum oven.

2.3. Physicochemical characterization of PAIHP

Fourier transform infrared (FTIR) spectrum (Perkin-Elmer Spectrophotometer Spectrum One) in the range 4000–450 cm^{-1} was studied. The morphological structure of the PAIHP was examined by scanning electron microscopy (SEM) using LEO 1455VP scanning microscope.

2.4. Adsorption procedure

The dye adsorption measurements were conducted by mixing of PAIHP in jars containing 250 mL of a dye solution (300 mg/L). The solution pH was adjusted by adding a small amount of H_2SO_4 or NaOH. The change on the absorbance of all solution samples were monitored and determined at certain time intervals during the adsorption process. At the end of the adsorption experiments, the solution samples were centrifuged and the dye concentration was determined. The results were verified with the adsorption kinetics and isotherms.

UV–VIS spectrophotometer CECIL 2021 was employed for absorbance measurements of samples. The maximum wavelengths (λ_{max}) used for determination of residual concentrations of DR31, DR23, DB22 and AB25 at pH 2 in supernatant solution using UV–VIS spectrophotometer were 527 nm, 503 nm, 478 nm and 605 nm, respectively.

The effect of adsorbent dosage on dye removal was investigated by contacting 250 mL of dye solution with initial dye concentration of 300 mg/L and pH 2 using jar test at room temperature (25 °C) for 60 min at a constant stirring speed of 200 rpm. Different amounts of PAIHP (0.005–0.020 g) were applied to remove dyes.

The effect of pH on dye removal was investigated by contacting 250 mL of dye solution with PAIHP (0.020 g) and initial dye concentration (300 mg/L) using jar test at room temperature (25 °C) for 60 min at a constant stirring speed of 200 rpm. Different pH values (2, 5, 8 and 10) were applied to remove dyes.

The effect of salt (0.02 M) on dye removal was investigated by contacting 250 mL of dye solution (300 mg/L) with PAIHP (0.020 g) and pH 2 using jar test at room temperature (25 °C) for 60 min at a constant stirring speed of 200 rpm. Different salts ($NaHCO_3$, Na_2CO_3 and Na_2SO_4) were used.

2.5. Dye desorption and PAIHP regeneration studies

The PAIHP used for the adsorption of 300 mg/L of dye solution was separated from the solution by centrifugation and dried. Then the adsorbent was agitated with 250 mL of distilled water at different pH values (2–12) for 60 min. The desorbed dye was determined.

To regenerate the PAIHP, the dye adsorbed adsorbent was poured into basic distilled water. Dye desorbed from the PAIHP. Then an organic solvent was added to solute the polymeric adsorbent. Organic phase containing PAIHP was separated from the aqueous phase containing the dye molecules. Finally, organic solvent was evaporated and the regenerated PAIHP was obtained.

3. Results and discussion

3.1. Characterization of PAIHP

In order to investigate the surface characteristics of PAIHP, FTIR and SEM image were studied. The FTIR spectrum of the PAIHP displays a number of characteristic bands (Fig. 3). The bands at 3443 cm^{-1}, 2949 cm^{-1}, 2838 cm^{-1}, 1643 cm^{-1}, 1382 cm^{-1} and 1152 cm^{-1} are assigned to stretching mode of the amino group (N–H), asymmetric stretching mode of the –CH$_2$– group, symmetric stretching mode of the –CH$_2$– group, stretching mode of the imide group, bending mode of –CH$_2$– group and stretching mode of the C–N, respectively [21].
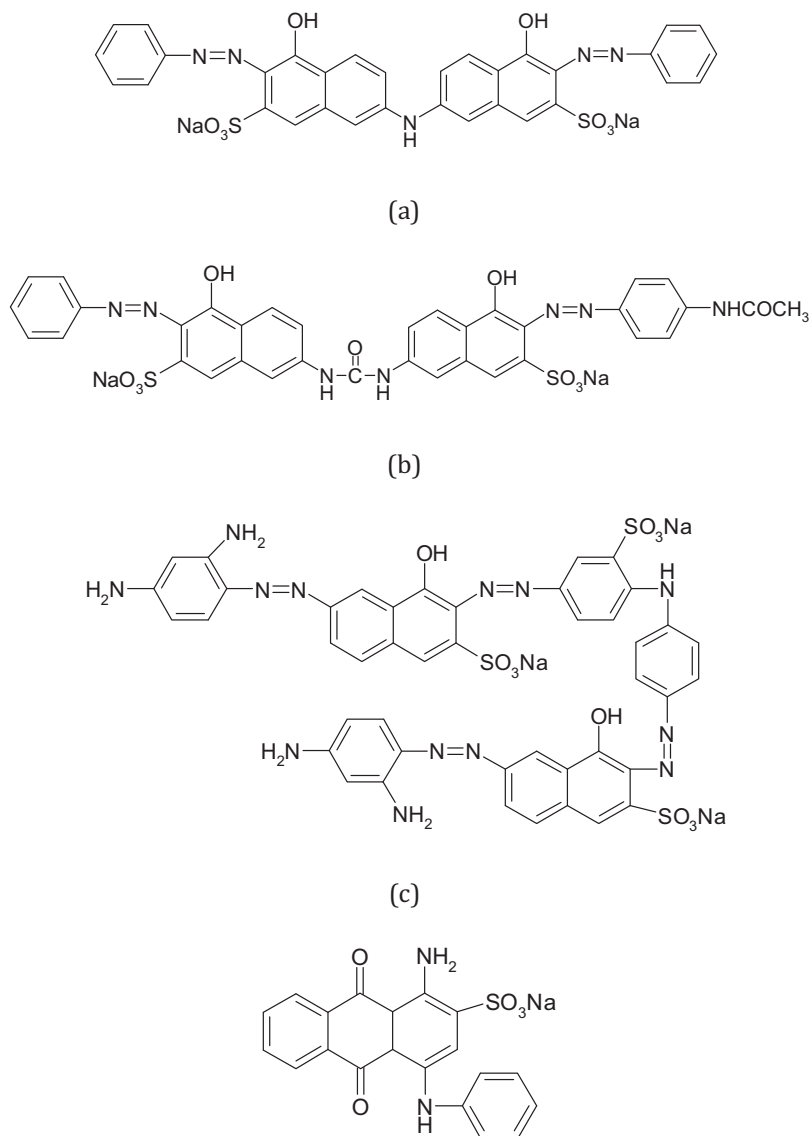
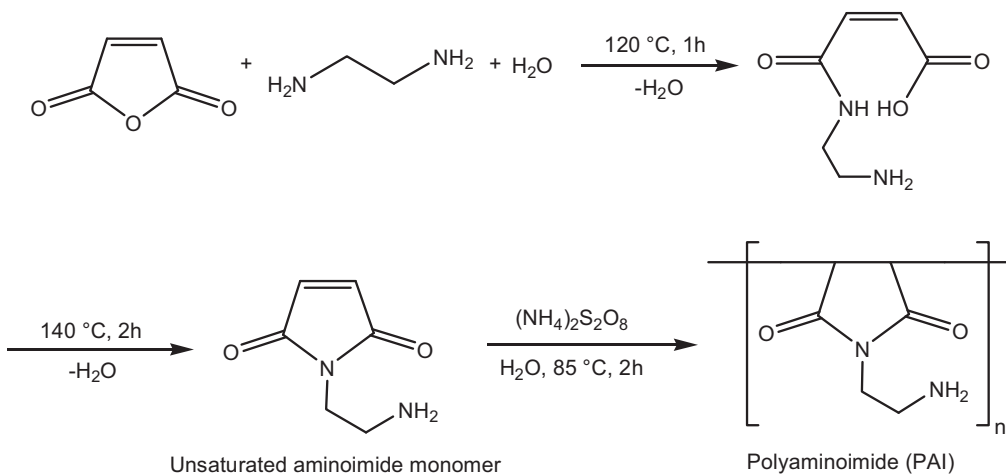**Fig. 1.** The chemical structure of dyes (a) DR31, (b) DR23, (c) DB22 and (d) AB25.
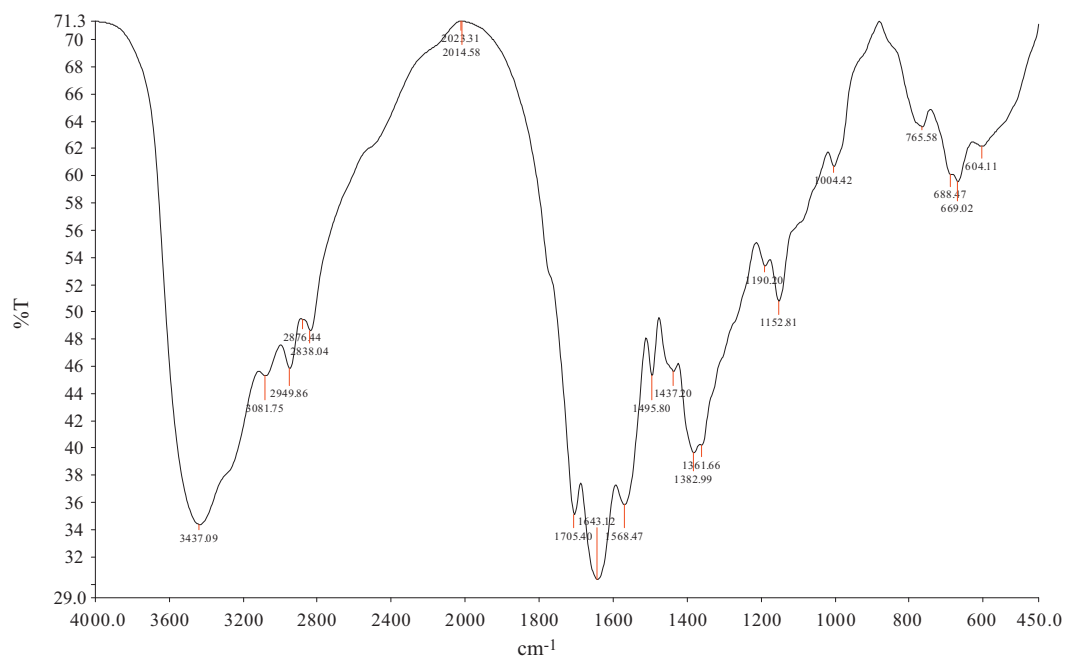

Fig. 2. The synthesis method of PAIHP.
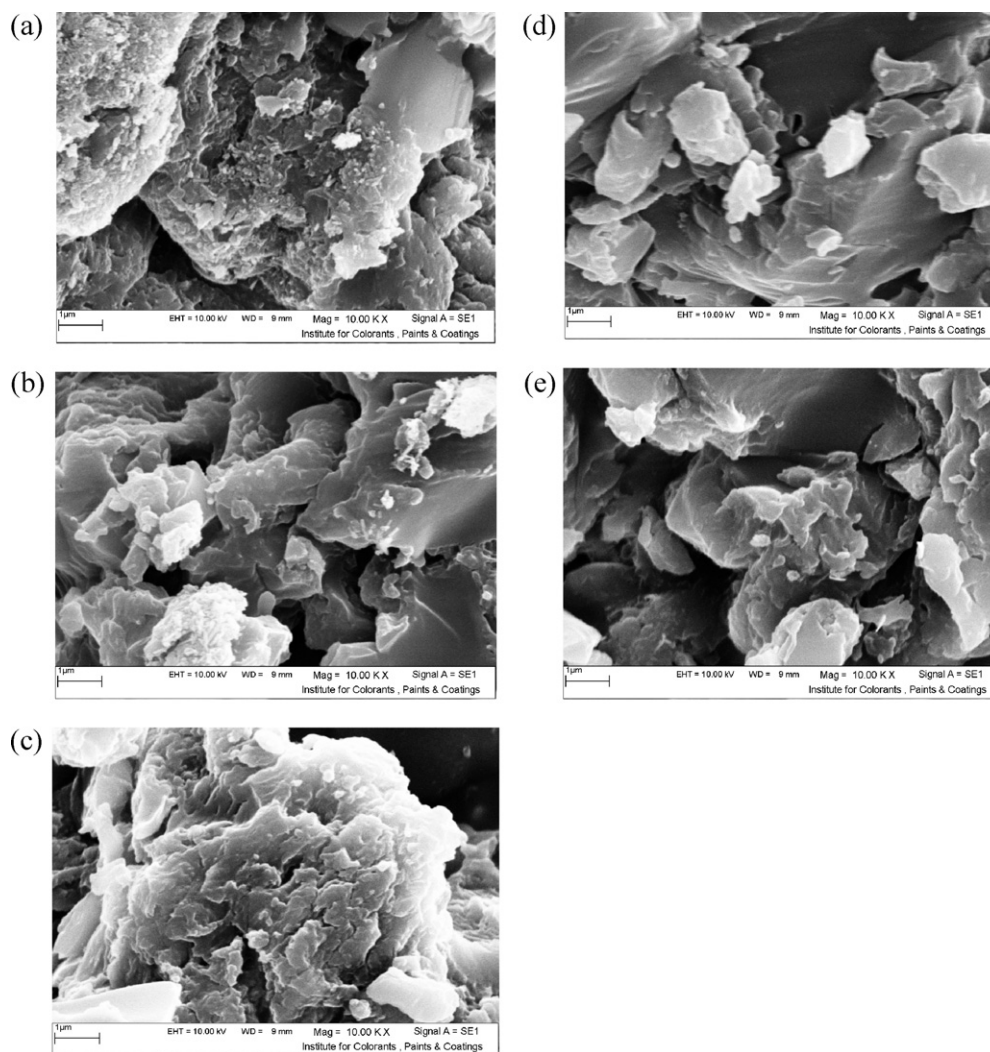
Fig. 3. FT-IR spectrum of PAIHP.

Fig. 4. SEM images (a) PAIHP, (b) DR31 adsorbed PAIHP, (c) DR23 adsorbed PAIHP, (d) DB22 adsorbed PAIHP and (e) AB25 adsorbed PAIHP.

Table 2
Linearized kinetic coefficients for dye adsorption onto PAIHP at different adsorbent dosages.

Dye	Adsorbent dosage	$(q_e)_{Exp}$	Pseudo-first order			Pseudo-second order			Intraparticle diffusion		
			$(q_e)_{Cal.}$	k_1	R^2	$(q_e)_{Cal.}$	k_2	R^2	k_p	I	R^2
DR31	0.0050	6246	1033	0.0585	0.6744	6250	0.0004	1	95	5536	0.9505
	0.0100	5311	1060	0.0550	0.6945	5263	0.0020	1	100	4549	0.9537
	0.0150	4270	166	0.0748	0.5104	4347	0.0020	1	11	4193	0.8970
	0.0200	3568	98	0.0889	0.5446	3571	0.0090	1	6	3527	0.8419
DR23	0.0050	4981	1424	0.0737	0.8650	5000	0.0002	1	163	3899	0.8943
	0.0100	4417	745	0.0737	0.7697	4347	0.0004	1	71	3932	0.9292
	0.0150	3715	315	0.0772	0.6603	3704	0.0015	1	24	3549	0.9669
	0.0200	3413	117	0.1034	0.6494	3448	0.0045	1	7	3369	0.9190
DB22	0.0050	7998	759	0.0852	0.7180	8333	0.0003	1	68	7558	0.8531
	0.0100	6216	807	0.1055	0.8393	6250	0.0008	1	71	5773	0.8600
	0.0150	4471	316	0.0871	0.6731	4545	0.0010	1	27	4295	0.8201
	0.0200	3622	374	0.0912	0.7595	3571	0.0013	1	32	3416	0.8972
AB25	0.0050	5150	1377	0.0822	0.8220	5263	0.0002	1	217	3830	0.7350
	0.0100	4468	186	0.0928	0.6189	4545	0.0020	1	15	4376	0.7931
	0.0150	3770	346	0.0873	0.7237	3846	0.0015	1	29	3579	0.8950
	0.0200	3328	270	0.0999	0.7441	3333	0.0018	1	25	3175	0.7593

SEM is an important tool to characterize the surface morphology and physical properties of the adsorbent surface. It is useful to determine the particle shape, porosity and appropriate size distribution of the adsorbent. Scanning electron micrographs of PAIHP and dye adsorbed PAIHP are shown in Fig. 4.

3.2. Adsorption kinetic

In order to study the mechanism of pollutant adsorption onto an adsorbent, characteristic constants of sorption were determined using pseudo-first order equation [22], pseudo-second order equation [23] and intraparticle diffusion [24–26].

A linear form of pseudo-first order model (Eq. (1)) is:

$$\log(q_e - q_t) = \log(q_e) - \left(\frac{k_1}{2.303}\right) t \tag{1}$$

where q_e, q_t and k_1 are the amount of dye adsorbed at equilibrium (mg/g), the amount of dye adsorbed at time t (mg/g) and the equilibrium rate constant of pseudo-first order kinetics (1/min), respectively. The linear fit between the $\log(q_e - q_t)$ and contact time (t) at pH 2 can be approximated as pseudo-first order kinetics.

Linear form of pseudo-second order model (Eq. (2)), was illustrated as:

$$\frac{t}{q_t} = \frac{1}{k_2 q_e^2} + \left(\frac{1}{q_e}\right) t \tag{2}$$

where k_2 is the equilibrium rate constant of pseudo-second order (g/mg min).

The possibility of intraparticle diffusion resistance affecting adsorption was explored by using the intraparticle diffusion model as

$$q_t = k_p t^{1/2} + I \tag{3}$$

where k_p and I are the intraparticle diffusion rate constant and intercept, respectively.

The plot of uptake should be linear when intraparticle diffusion is involved in the adsorption process. In addition, intraparticle diffusion is the rate controlling step when the lines of uptake pass through the origin. When the plots do not pass through the origin, this is indicative of some degree of boundary layer control and it shows that the intraparticle diffusion is not the only rate limiting step, but also other kinetic models may control the rate of adsorption, all of which may be operating simultaneously [24–26].

To understand the applicability of the pseudo first-order, pseudo second-order and intra-particle diffusion models for the dye adsorption onto PAIHP at different adsorbent dosage, linear plots of $\log(q_e - q_t)$ versus contact time (t), t/q_t versus contact time (t) and q_t against $t^{1/2}$ are plotted. The values of k_1, k_2, k_p, I, R^2 (correlation coefficient values) and the calculated q_e ($(q_e)_{Cal.}$) are shown in Table 2.

The linearity of the plots (R^2) demonstrates that pseudo-first order and intraparticle diffusion kinetic models do not play a significant role in the uptake of the dye (Table 2). The linear fit between the t/q_t versus contact time (t) and calculated correlation coefficients (R^2) for pseudo-second order kinetics model show that the dye removal kinetic can be approximated as pseudo-second order kinetics (Table 2). In addition, the experimental q_e ($(q_e)_{Exp.}$) values agree with the calculated ones ($(q_e)_{Cal.}$), obtained from the linear plots of pseudo-second order kinetics (Table 2).

3.3. Adsorption isotherm

The adsorption isotherm investigates the relation between the mass of the dye adsorbed onto adsorbent and liquid phase of the dye concentration [27,28]. Several isotherms such as Langmuir, Freundlich and Tempkin models were studied in details.

In Langmuir isotherm, a basic assumption is that sorption takes place at specific sites within the adsorbent [29–32]. The Langmuir equation can be written as follows:

$$q_e = Q_0 K_L C_e / (1 + K_L C_e) \tag{4}$$

Table 3
Linearized isotherm coefficients for dye adsorption onto PAIHP at different adsorbent dosages.

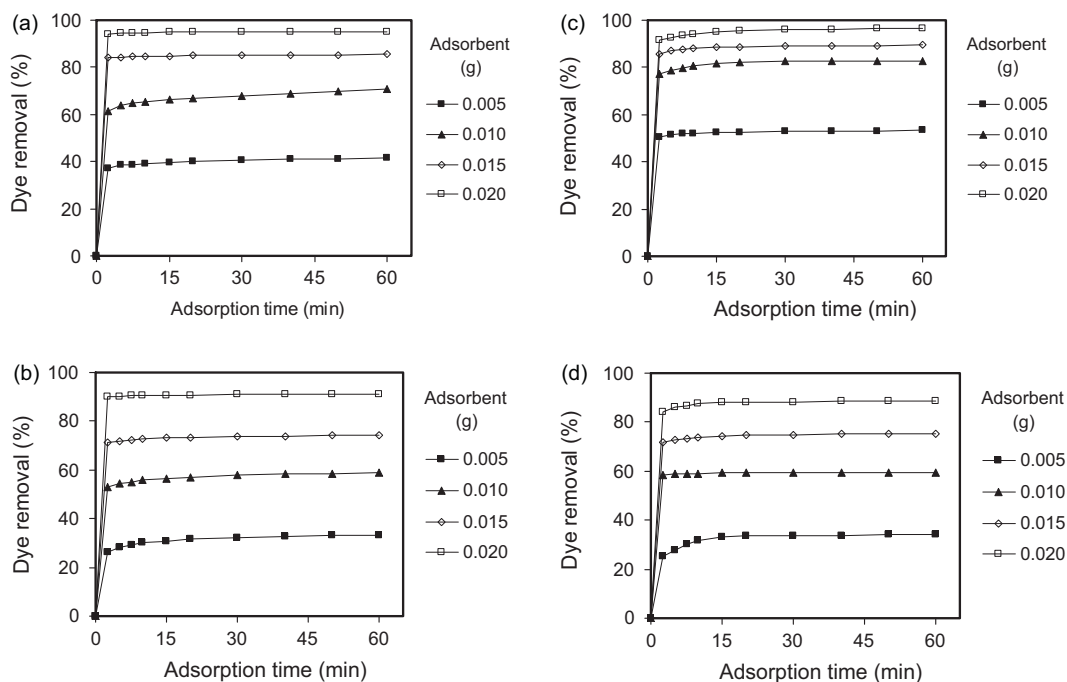| Dye	Langmuir			Freundlich			Tempkin		
	Q_0	K_L	R^2	K_F	$1/n$	R^2	K_T	B_1	R^2
DR31	6667	0.0333	0.9917	1883	0.2295	0.9822	1.541375	142	0.9627
DR23	5555	0.0426	0.9846	1771	0.1885	0.9012	2.482521	773	0.8801
DB22	9090	0.0370	0.9828	1678	0.3150	0.9513	0.643453	1729	0.9331
AB25	5882	0.0345	0.9882	1345	0.2503	0.9710	0.644395	1035	0.9518

Fig. 5. The effect of adsorbent dosage on dye removal by PAIHP (a) DR31 and (b) DR23 (c) DB22 and (d) AB25.

where q_e, C_e, K_L and Q_0 are the dye concentration at equilibrium (mg/L), Langmuir constant (L/g) and the maximum adsorption capacity (mg/g), respectively.

The linear form of Langmuir equation is:

$$\frac{C_e}{q_e} = \frac{1}{K_L Q_0} + \frac{C_e}{Q_0} \quad (5)$$

Also, Isotherm data were tested with Freundlich isotherm that can be expressed by [29,33]:

$$q_e = K_F C_e^{1/n} \quad (6)$$

where K_F is adsorption capacity at unit concentration and $1/n$ is adsorption intensity.

Eq. (6) can be rearranged to a linear form:

$$\log q_e = \log K_F + \frac{1}{n} \ \log C_e \quad (7)$$

The Tempkin isotherm is given as:

$$q_e = \frac{RT}{b} \ \ln(K_T C_e) \quad (8)$$

which can be linearized as:

$$q_e = B_1 \ \ln K_T + B_1 \ \ln C_e \quad (9)$$

where

$$B_1 = \frac{RT}{b} \quad (10)$$

Tempkin isotherm assumes that the heat of adsorption of all the molecules in the layer decreases linearly with coverage due to adsorbent–adsorbate interactions. Also, the adsorption is characterized by a uniform distribution of binding energies, up to some maximum binding energy [34,35]. A plot of q_e versus $\ln C_e$ enables the determination of the isotherm constants B_1 and K_T from the slope and the intercept, respectively. K_T is the equilibrium binding constant (L/mg) corresponding to the maximum binding energy and constant B_1 is related to the heat of adsorption.

To study the applicability of the Langmuir, Freundlich and Tempkin isotherms for the dye adsorption onto PAIHP at different adsorbent dosage, linear plots of C_e/q_e against C_e, $\log q_e$ versus

$\log C_e$ and q_e versus $\ln C_e$ are plotted. The values of Q_0, K_L, K_F, $1/n$, K_T, B_1 and R^2 (correlation coefficient values of all isotherms models) are shown in Table 3.

The R^2 values show that the dye removal isotherm using PAIHP does not follow the Freundlich and Tempkin isotherms (Table 3). The linear fit between the C_e/q_e versus C_e and R^2 values for Langmuir isotherm model show that the dye removal isotherm can be approximated as Langmuir model (Table 3). This means that the adsorption of dyes takes place at specific homogeneous sites and a one layer adsorption onto PAIHP surface.

3.4. Effect of operational parameter on dye removal

3.4.1. Effect of PAIHP dosage

The plot of dye removal (%) versus time (min) at different PAIHP dosages (g) was shown in Fig. 5.

The increasing of dye adsorption with adsorbent dosage can be attributed to increased adsorbent surface and availability of more adsorption sites. However, the capacity decreased with the increasing amount of adsorbent when the adsorption capacity was expressed in mg adsorbed per gram of material. It can be attributed to overlapping or aggregation of adsorption sites resulting in a decrease in total adsorbent surface area available to the dye and an increase in diffusion path length [36].

3.4.2. Effect of pH

The effect of pH on the adsorption of dyes onto PAIHP is shown in Fig. 6. The adsorption capacity increases when the pH decreases. Maximum adsorption of anionic dyes occurs at acidic pH (pH 2). At various pH values, the electrostatic attraction as well as the organic property and structure of dye molecules and PAIHP could play very important roles in dye adsorption on PAIHP. At acidic pH values, amino functional groups of polymer protonate. At pH 2, a significantly high electrostatic attraction exists between the positively charged ($-NH_3^+$) surface of the PAIHP and negatively charged anionic dye [37]. As the pH of the system increases, the number of positively charged sites decreased. It does not favor the adsorption of anionic dyes onto PAIHP. The effective pH was 2 and it was used in further studies.
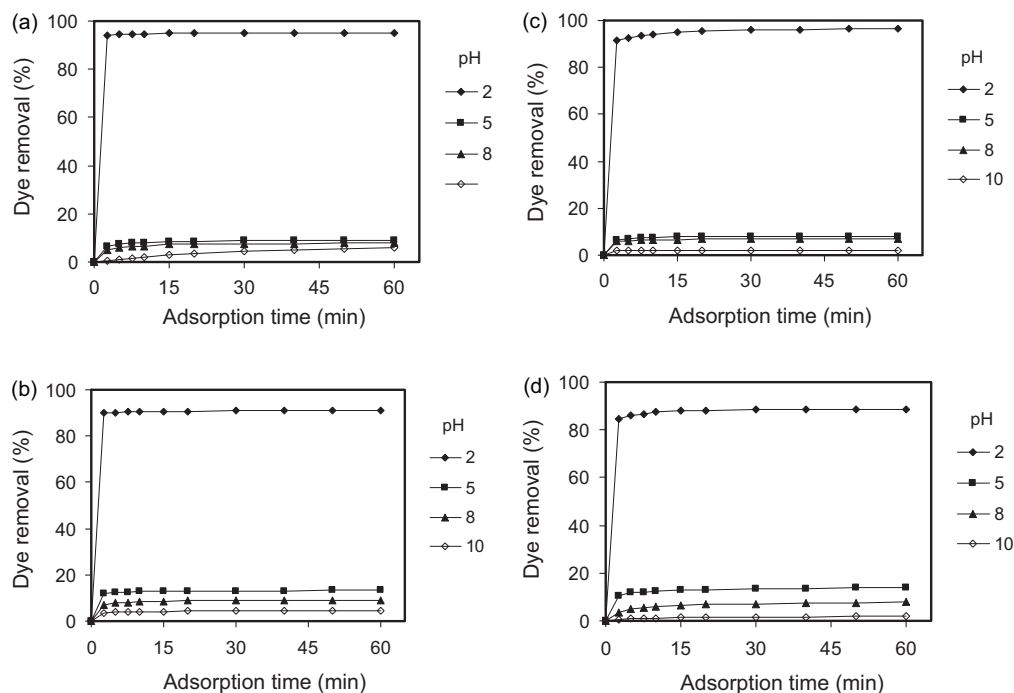
Fig. 6. The effect of pH on dye removal by PAIHP (a) DR31 and (b) DR23 (c) DB22 and (d) AB25.

3.4.3. Effect of salt

The occurrence of salts is rather common in colored wastewater [38]. Inorganic anions of salts may compete for the active sites on the adsorbent surface or deactivate the adsorbent. Thus dye adsorption efficiency decreases. An important limitation resulting from the high reactivity and non-selectivity of adsorbent is that it also reacts with non-target compounds present in the wastewater such as dye auxiliaries present in the exhausted reactive dye bath. It results higher adsorbent dosage demand to accomplish the desired degree of dye removal efficiency.

To investigate inorganic salts effect on dye removal efficiency, 0.02 M of $NaHCO_3$, Na_2CO_3 and Na_2SO_4 were used. Fig. 7 illustrates that dye removal capacity of PAIHP decreases in the presence of inorganic salts because these salts have small molecules and compete with dyes in adsorption by PAIHP.

3.5. Desorption studies

The regeneration of the adsorbent is one of the important factors to the economical treatment process. Desorption studies help
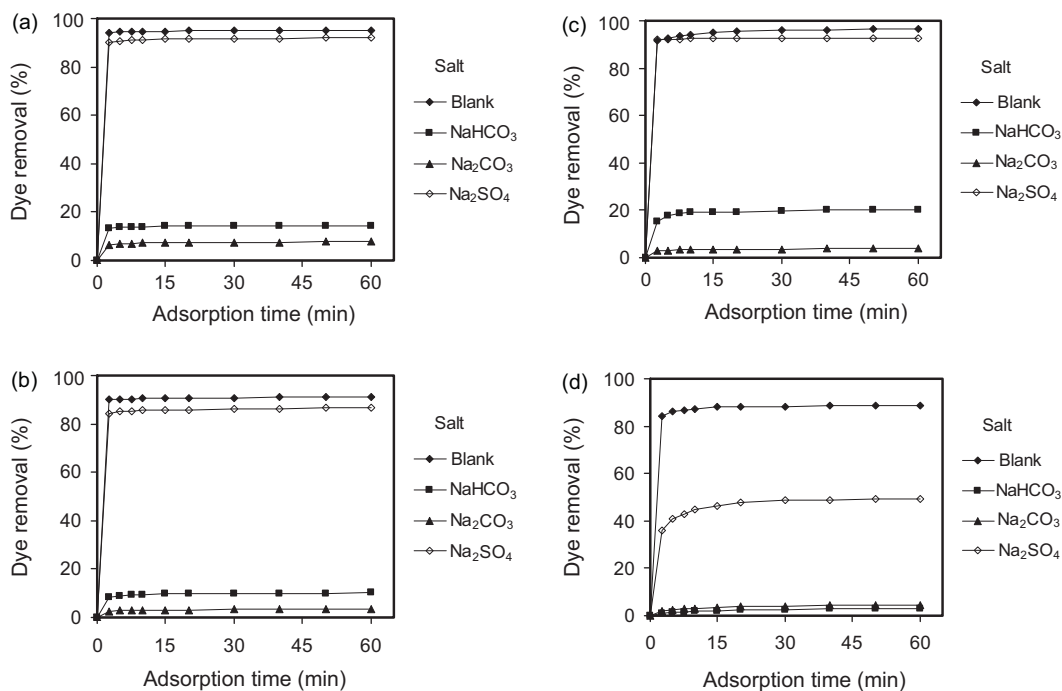

Fig. 7. The effect of salt on dye removal by PAIHP (a) DR31 and (b) DR23 (c) DB22 and (d) AB25.
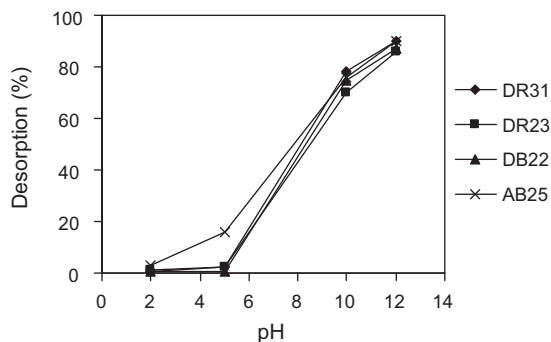
Fig. 8. Desorption of dyes from PAIHP at different pH values.

to recovery of the adsorbate and adsorbent. Dye desorption tests showed that the maximum dye release of 90% for DR31, 86% for DR23, 87% for DB22 and 90% for AB25 were achieved in aqueous solution at pH 12 (Fig. 8). At high pH value, the number of positively charged sites decreases which favors desorption of dyes and regeneration of adsorbent [39].

4. Conclusion

In this paper, PAIHP was synthesized and its dye removal abilities were investigated. Direct Red 31 (DR31), Direct Red 23 (DR23), Direct Black 22 (DB22) and Acid Blue 25 (AB25) were used as model compounds. Adsorption kinetic of dyes was found to conform to pseudo-second order kinetics. It was found that dye adsorption onto PAIHP followed with Langmuir isotherm. At a fixed PAIHP dosage, the dye removal increases with decreasing pH. Dye removal capacity of PAIHP decreases in the presence of inorganic salts. PAIHP was regenerated at pH 12. The results showed that the PAIHP, a polymeric adsorbent with high dye adsorption capacity, might be a suitable alternative to remove dyes from colored wastewater.

References

[1] A.Y. Zahrim, C. Tizaoui, N. Hilal, Coagulation with polymers for nanofiltration pre-treatment of highly concentrated dyes: a review, Desalination 266 (2011) 1–16.
[2] N.M. Mahmoodi, Photocatalytic ozonation of dyes using copper ferrite nanoparticle prepared by co-precipitation method, Desalination 279 (2011) 332–337.
[3] N.M. Mahmoodi, B. Hayati, M. Arami, H. Bahrami, Preparation, characterization and dye adsorption properties of biocompatible composite (alginate/titania nanoparticle), Desalination 275 (2011) 93–101.
[4] E. Forgacs, T. Cserhati, G. Oros, Removal of synthetic dyes from wastewaters: a review, Environ. Int. 30 (2004) 953–971.
[5] Z. Aksu, Application of biosorption for the removal of organic pollutants: a review, Process Biochem. 40 (2005) 997–1026.
[6] N.M. Mahmoodi, Equilibrium, kinetic and thermodynamic of dye removal using alginate from binary system, J. Chem. Eng. Data 56 (2011) 2802–2811.
[7] N.M. Mahmoodi, R. Salehi, M. Arami, Binary system dye removal from colored textile wastewater using activated carbon: kinetic and isotherm studies, Desalination 272 (2011) 187–195.
[8] N.M. Mahmoodi, R. Salehi, M. Arami, H. Bahrami, Dye removal from colored textile wastewater using chitosan in binary systems, Desalination 267 (2011) 64–72.
[9] N.M. Mahmoodi, B. Hayati, M. Arami, Textile dye removal from single and ternary systems using date stones: kinetic, isotherm and thermodynamic studies, J. Chem. Eng. Data 55 (2010) 4638–4649.
[10] N.M. Mahmoodi, M. Arami, H. Bahrami, S. Khorramfar, Novel biosorbent (Canola hull): surface characterization and dye removal ability at different cationic dye concentrations, Desalination 264 (2010) 134–142.
[11] N. Atar, A. Olgun, F. Çolak, Thermodynamic, equilibrium and kinetic study of the biosorption of Basic Blue 41 using Bacillus macerans, Eng. Life Sci. 8 (2008) 499–506.
[12] Y. Bulut, H. Aydin, A kinetics and thermodynamics study of methylene blue adsorption on wheat shells, Desalination 194 (2006) 259–267.
[13] H. Parab, M. Sudersanan, N. Shenoy, T. Pathare, B. Vaze, Use of agro-industrial wastes for removal of basic dyes from aqueous solutions, Clean 37 (2009) 963–969.
[14] B. Pan, B. Pan, W. Zhang, L. Lv, Q. Zhang, S. Zheng, Development of polymeric and polymer-based hybrid adsorbents for pollutants removal from waters, Chem. Eng. J. 151 (2009) 19–29.
[15] B.C. Pan, Q.X. Zhang, F.W. Meng, X.T. Li, X. Zhang, J.Z. Zheng, W.M. Zhang, B.J. Pan, J.L. Chen, Sorption enhancement of aromatic sulfonates onto an aminated hyper-cross-linked polymer, Environ. Sci. Technol. 39 (2005) 3308–3313.
[16] K. Zheng, B.C. Pan, Q.J. Zhang, W.M. Zhang, B.J. Pan, Y.H. Han, Q.R. Zhang, W. Du, Z.W. Xu, Q.X. Zhang, Enhanced adsorption of p-nitroaniline from water by a carboxylated polymeric adsorbent, Sep. Purif. Technol. 57 (2007) 250–256.
[17] G. Bayramoglu, B. Altintas, M.Y. Arica, Adsorption kinetics and thermodynamic parameters of cationic dyes from aqueous solutions by using a new strong cation-exchange resin, Chem. Eng. J. 152 (2009) 339–346.
[18] X. Zhang, A. Li, Z. Jiang, Q. Zhang, Adsorption of dyes and phenol from water on resin adsorbents: effect of adsorbate size and pore size distribution, J. Hazard. Mater. 137 (2006) 1115–1122.
[19] Y. Yu, Y.Y. Zhuang, Z.H. Wang, Adsorption of water-soluble dye onto functionalized resin, J. Colloid Interface Sci. 242 (2001) 288–293.
[20] L.G.T. dos Reis, N.F. Robaina, W.F. Pacheco, R.J. Cassella, Separation of Malachite Green and Methyl Green cationic dyes from aqueous medium by adsorption on Amberlite XAD-2 and XAD-4 resins using sodium dodecyl sulfate as carrier, Chem. Eng. J. (2011), doi:10.1016/j.cej.2011.04.024.
[21] D.L. Pavia, G.M. Lampman, G.S. Kaiz, Introduction to Spectroscopy: A Guide for Students of Organic Chemistry, W.B. Saunders Company, 1987.
[22] S. Lagergren, Zur theorie der sogenannten adsorption geloster stoffe, K. Sven. Vetenskapsakad. Handl. 24 (1898) 1–39.
[23] Y.S. Ho, Adsorption of heavy metals from waste streams by peat, PhD Thesis, The University of Birmingham, Birmingham, UK, 1995.
[24] A. Ozcan, A.S. Ozcan, Adsorption of Acid Red 57 from aqueous solutions onto surfactant-modified sepiolite, J. Hazard. Mater. 125 (2005) 252–259.
[25] S. Senthilkumaar, P. Kalaamani, K. Porkodi, P.R. Varadarajan, C.V. Subburaam, Adsorption of dissolved reactive red dye from aqueous phase onto activated carbon prepared from agricultural waste, Bioresour. Technol. 97 (2006) 1618–1625.
[26] W.J. Weber, J.C. Morris, Kinetics of adsorption on carbon from solution, J. Sanitary Eng. Div. Am. Soc. Civil Eng. 89 (1963) 31–60.
[27] M. Uğurlu, Adsorption of a textile dye onto activated sepiolite, Micropor. Mesopor. Mater. 119 (2009) 276–283.
[28] E. Demirbas, M. Kobya, S. Oncel, S. Sencan, Removal of Ni(II) from aqueous solution by adsorption onto hazelnut shell activated carbon: equilibrium studies, Bioresour. Technol. 84 (2002) 291–293.
[29] N.K. Amin, Removal of reactive dye from aqueous solutions by adsorption onto activated carbons prepared from sugarcane bagasse pith, Desalination 223 (2008) 152–161.
[30] I. Langmuir, The constitution and fundamental properties of solids and liquids. I. Solids, J. Am. Chem. Soc. 38 (1916) 2221–2295.
[31] I. Langmuir, The constitution and fundamental properties of solids and liquids. II. Liquids, J. Am. Chem. Soc. 39 (1917) 1848–1906.
[32] I. Langmuir, The adsorption of gases on plane surfaces of glass, mica and platinum, J. Am. Chem. Soc. 40 (1918) 1361–1403.
[33] H.M.F. Freundlich, Uber die adsorption in lasugen, Z. Phys. Chem. (Leipzig) 57A (1906) 385–470.
[34] M.J. Tempkin, V. Pyzhev, Recent modification to Langmiur isotherms, Acta Physiochim. USSR 12 (1940) 217–222.
[35] Y.C. Kim, I. Kim, S.C. Rengraj, J. Yi, Arsenic removal using mesoporous alumina prepared via a templating method, Environ. Sci. Technol. 38 (2004) 924–931.
[36] G. Crini, C. Robert, F. Gimbert, B. Martel, O. Adam, F. De Giorgi, The removal of Basic Blue 3 from aqueous solutions by chitosan-based adsorbent: batch studies, J. Hazard. Mater. 153 (2008) 96–106.
[37] M.N.V.R. Kumar, A review of chitin and chitosan applications, React. Funct. Polym. 46 (2000) 1–27.
[38] N.M. Mahmoodi, M. Arami, J. Zhang, Preparation and photocatalytic activity of immobilized composite photocatalyst (titania nanoparticle/activated carbon), J. Alloys Compd. 509 (2011) 4754–4764.
[39] N.M. Mahmoodi, B. Hayati, M. Arami, F. Mazaheri, Single and binary system dye removal from colored textile wastewater by a dendrimer as a polymeric nanoarchitecture: equilibrium and kinetics, J. Chem. Eng. Data 55 (2010) 4660–4668.